

Letter pubs.acs.org/journal/aidcbc

Pyochelin Biosynthetic Metabolites Bind Iron and Promote Growth in Pseudomonads Demonstrating Siderophore-like Activity

Anna R. Kaplan,[‡] Djamaladdin G. Musaev, and William M. Wuest*



Cite This: ACS Infect. Dis. 2021, 7, 544-551



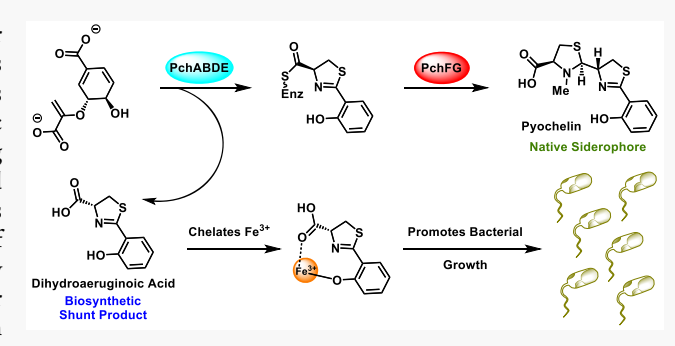
ACCESS I

Metrics & More



Supporting Information

ABSTRACT: Pseudomonads employ several strategies to sequester iron vital for their survival including the use of siderophores such as pyoverdine and pyochelin. Similar in structure but significantly less studied are pyochelin biosynthetic byproducts, dihydroaeruginoic acid, aeruginoic acid, aeruginaldehyde (IQS), and aeruginol, along with two other structurally related molecules, aerugine and pyonitrins A-D, which have all been isolated from numerous Pseudomonad extracts. Because of the analogous substructure of these compounds to pyochelin, we hypothesized that they may play a role in iron homeostasis or have a biological effect on other bacterial species. Herein, we discuss the physiochemical evaluation of these molecules and disclose, for the first time, their ability to bind iron and promote growth in Pseudomonads.



KEYWORDS: iron acquisition, Pseudomonas aeruginosa, siderophores, pyochelin

ron plays a critical role in a variety of biological functions, from electron transport pathways to metalloenzyme cofactors, making it vital for the growth and survival of aerobic bacteria. In environments such as the rhizosphere, the region directly surrounding the root of a plant, bacteria compete for limited essential resources as a means of survival.² Iron is most commonly taken up by bacteria in ferric (Fe^{II}) or ferrous (Fe^{III}) forms. In aerobic environments, including the rhizosphere, iron is commonly present as a highly insoluble ferric oxide complex (Fe₂O₃), the stability of which limits the bioavailable Fe^{III} concentration to 10⁻⁹ to 10⁻¹⁸ M, far below the concentration of 10⁻⁶ M required for bacterial survival. Further, in host organisms, the majority of Fe^{III} is sequestered in heme or circulating proteins, limiting the free ${\rm Fe^{III}}$ concentration to 10^{-24} M. $^{3-5}$ Thus, despite being the fourth most abundant element on earth, iron acquisition presents a unique challenge for bacterial survival.

Bacteria have evolved several different iron uptake strategies including, but not limited to, direct uptake of iron-bound proteins like ferritin, secretion of hemophores, and most commonly, the use of siderophores and xenosiderophores.^{3,4} Siderophores are small molecules that chelate extracellular Fe^{III}, forming complexes that are selectively reimported back into cells. By a similar mechanism, xenosiderophores, which are not produced by the bacterium itself, are also taken up into cells using similar receptors.⁶ In both cases, specific transport machinery is required to import the Fe^{III}-chelated complexes into the cell. These molecules commonly contain at least one of five structural moieties that contribute to their iron-chelating ability; hydroxamate, phenolate, catecholate, carboxylate, and

oxazoline/thiazoline heterocycles.3,4,7,8 While many siderophores such as enterobactin, desferrioxamine B, and staphyloferrin employ a single motif to bind iron, others are mixed-type, employing multiple iron-binding moieties.^{3,4} This is best exemplified by those produced by various Gramnegative pathogens, including Pseudomonads, which combine the phenolate/catecholate moiety with oxazolines/thiazolines and have been of particular interest to our research group (Figure 1A).

Pseudomonads produce a variety of metabolites including antibiotics and siderophores, giving them a competitive advantage in densely populated environments. 9,10 Like many pathogenic bacteria, Pseudomonas aeruginosa, often found in the lungs of cystic fibrosis patients, 11 produce two different siderophores, high-affinity pyoverdine, and lower-affinity pyochelin (Figure 1B).6 Their production levels are highly regulated by the ferric uptake regulatory (Fur) system, which senses the amount of bioavailable extracellular iron levels to promote transcription of the appropriate biosynthetic machinery. 12 Because of the long-standing interest our group has had in pyochelin-like natural products 93,14 as well as other iron-binding *Pseudomonad* antibiotics, 15-18 we wanted to inves-

Received: December 21, 2020 Published: February 12, 2021





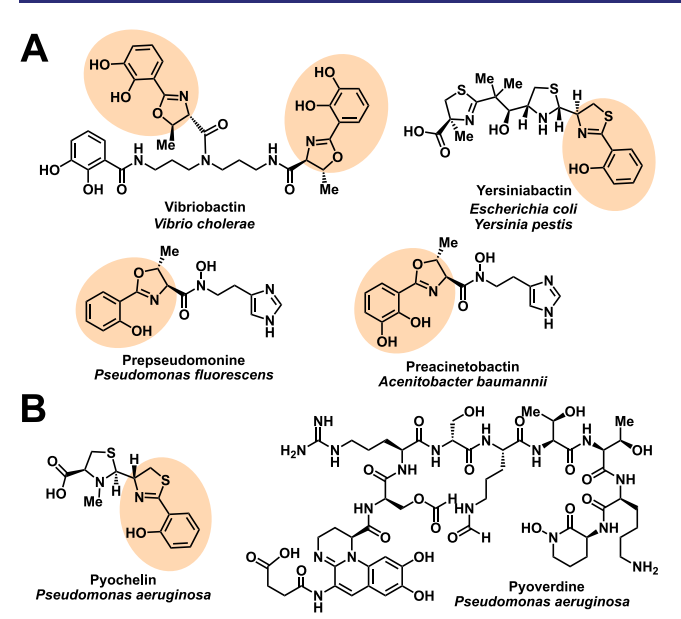


Figure 1. (A) Structures of siderophores containing both a phenolate/catecholate motif and an oxazoline/thiazoline and corresponding producing organisms; (B) structures of *P. aeruginosa* siderophores, pyochelin and pyoverdine. ^{3,4,7,8}

tigate a series of pyochelin biosynthetic shunt products and their ability to sequester iron or influence bacterial growth.

Like many siderophores, biosynthesis of pyochelin is orchestrated via nonribosomal peptide synthetases (NRPSs).^{7,8} As shown in Figure 2A, chorismate is first converted to salicylate by the two accessory enzymes, PchA and PchB. Salicylate is then activated by PchD, loaded to PchE, and condensed with one molecule of L-cysteine, cyclized, and epimerized. Another cysteine molecule is incorporated by PchF, after which the tailoring protein, PchG, reduces this

second thiazoline to a thiazolidine, which is then *N*-methylated. Pyochelin is then released from the biosynthetic machinery and exported to sequester iron. PchC, a thioesterase, has been shown to cleave PchE-appended salicylate, resulting in the accumulation of dihydroaeruginoic acid (Dha, 1), which can then be further converted to aeruginoic acid (2), aeruginaldehyde (also called IQS) (3), and aeruginol (4). State of the secondary metabolites may also be formed from other pathways.

While pyochelin is better characterized, physiochemical and biological properties of these simpler biosynthetic shunt products are largely unknown. Dha (1) was initially characterized as an iron-chelating, antiproliferative compound;²⁴ however, these iron-chelating properties were not extensively investigated. Dha was also found to have modest antifungal and antibacterial activity, although the scope of microbes tested was quite limited. 25 Aeruginoic acid (2) 26 was isolated and synthesized by Yamada and co-workers in 1970, and aeruginol (4)²⁷ was isolated from a CHCl₃ extract of P. aeruginosa and structurally characterized in 1993. To the best of our knowledge, the properties of neither compound have been assessed further. Isolated from P. fluorescens, aerugine (5, Figure 2A) has limited antifungal activity; however, it too has not been further characterized.²⁸ IQS (3) has been isolated from multiple Pseudomonads and also displays modest antifungal activity. 21,29,30 There has been debate in the literature regarding its role in Pseudomonads. It has been coined "the fourth quorum sensing molecule" in P. aeruginosa;³¹ however, this claim has since been refuted.³² A key feature of IQS is the reactive aldehyde moiety, which facilitates its incorporation into the scaffolds of numerous natural products like mindapyrrole B³³ and malleonitrone²³ (Figure 2B). Clardy recently discovered the pyonitrins A-D (6, Figure 2A) from the extract of P. protegens. Assessment of the genome indicated that these metabolites arise from a spontaneous nonenzymatic Pictet-Spengler condensation

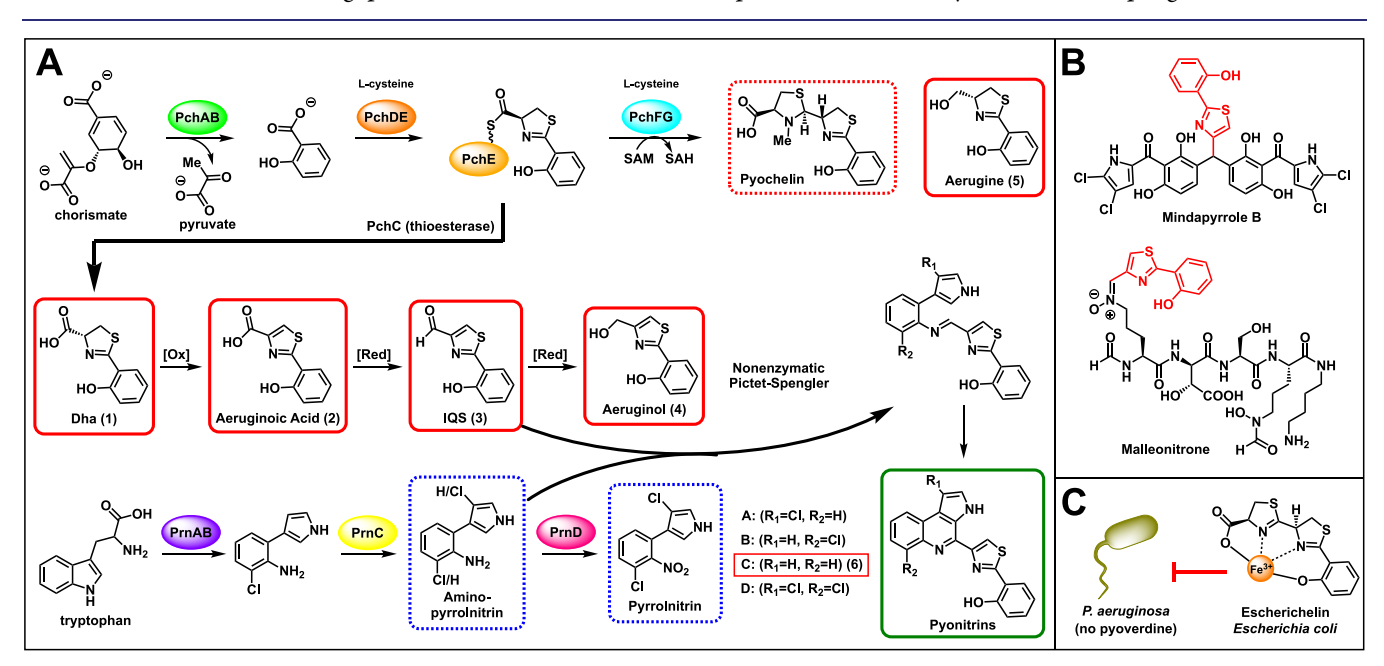


Figure 2. (A) Abbreviated biosynthetic pathways to siderophore pyochelin, antibiotic pyrrolnitrin in *P. aeruginosa*, and Dha (1), and nonenzymatic conversion to aeruginoic acid (2), IQS (3), and aeruginol (4); structure of aerugine (5) and spontaneous reaction of IQS with aminopyrrolnitrin to form pyonitrins A–D (6); $^{7,8,19-23,35,36}$ (B) structures of microbial metabolites featuring IQS incorporation; 23,34 (C) structure of yersiniabactin biosynthetic shunt product, escheriachelin, and its inhibition of pyoverdine-deficient *P. aeruginosa* growth through Fe^{III} chelation.

Scheme 1. Synthetic Conditions Employed to Access Dha (1), Aeruginoic Acid (2), IQS (3), Aeruginol (4), Aerugine (5), and Pyonitrin (6)^{26,36,43-45}

between IQS and aminopyrrolnitrin,²² a precursor to the known *Pseudomonad* antifungal, pyrrolnitrin.³⁴ This pathway was recently validated through the biomimetic total synthesis of the pyonitrins A–D by MacMillan and co-workers and the synthesis of pyonitrin C in this work.³⁵

With knowledge of these compounds being limited, we proposed that a directed investigation of their physiochemical and biological properties would provide further evolutionary insight into their origins. For example, do these metabolites play a role in iron homeostasis in P. aeruginosa or are they purely artifacts? As previously mentioned, production of pyochelin and pyoverdine is tightly regulated by the Fur system, likely evolved to save valuable resources thereby only producing pyoverdine, the more resource-intensive compound to biosynthesize, when iron is incredibly scarce. 12,36 Since Dha has been identified in the supernatant of iron-limited P. aeruginosa cells,³⁷ we reasoned that it may function as a simplified siderophore, as originally proposed by Reimmann and co-workers in 2014.³⁸ Alternatively, 1-6 could have a function similar to that of escherichelin (Figure 2C), a yersiniabactin shunt product found to inhibit pyochelinmediated iron uptake in pyoverdine-deficient P. aeruginosa.³⁹⁻⁴¹

With a series of unanswered questions regarding these metabolites, we sought to gain insight into their physiochemical and biological properties and their purpose in *P. aeruginosa*. Toward this end, we concisely synthesized compounds 1–6 using well predented protocols (Scheme 1). Aeruginoic acid (2) was synthesized in three steps according to the originally published route. ²⁶ 3-Hydroxybenzamide was converted to the corresponding thioamide (7), which was then condensed with ethyl bromopyruvate giving the corresponding thiazole (8). The ethyl ester was then hydrolyzed, furnishing aeruginoic acid (2). Subsequent reduction with BH₃·THF afforded aeruginol (4). Dha (1) was synthesized in one step by

condensing 2-hydroxybenzonitrile with L-cysteine, as previously described by Mislin. 42,43 Reduction of condensation product, 9, with NaBH₄ yielded aerugine (5), which was then oxidized directly to IQS (3) using Swern conditions.⁴² It should be noted that IQS (3) has also been accessed via a Weinreb amide intermediate, wherein the thiazoline is oxidized to the thiazole followed by Weinreb amide reduction to the aldehyde. 44 Evidently, we found it more efficient to access IQS (3) directly from aerugine (5). With the first five metabolites synthesized, we then turned our attention to the synthesis of aminopyrrolnitrin (14), the second precursor to the biomimetic Pictet-Spengler condensation reaction. Pyrrole was first protected with TIPS to give 10 in near quantitative yield. The bulky TIPS group then enabled regioselective iodination, yielding the desired 3-iodinated pyrrole, 11. Borylation followed by Suzuki-Miyaura coupling with 2-iodoaniline gave 13 in 85% yield over two steps. Deprotection with TBAF then afforded aminopyrrolnitrin (14).⁴⁵ The final Pictet-Spengler reaction was performed using conditions adapted from MacMillan and co-workers; after stirring in a 1% solution of TFA in DMSO for 24 h, IQS (3) and aminopyrrolnitrin (14) furnished pyonitrin (6).35 This synthetic result confirms the inherent reactivity these two substrates have toward each other, supporting the previously discussed biosynthesis of

With all 6 metabolites in hand, we began our assessment of their iron-chelating abilities. This was first evaluated qualitatively by adding increasing amounts to a solution of FeCl₃. In most cases, a distinct color change was observed, wherein the yellow solution of FeCl₃ in methanol turned darker shades of purple upon addition to solutions of each compound (Figure S1). There are some compounds, such as 6, for which the color change is not quite as distinct; thus, the quantitative approach described further was especially useful in confirming the iron-binding properties of these compounds.

These iron-chelating properties were then further quantified using fluorescence titration experiments. In these experiments, 0.1 equiv of Fe^{III} was added to a solution of a given compound in methanol, and an emission spectrum was recorded after each addition. The emission signals of all compounds were quenched by the addition of varying amounts of Fe^{III} (Figure 3A). Compounds 1 and 2 were also titrated with five additional

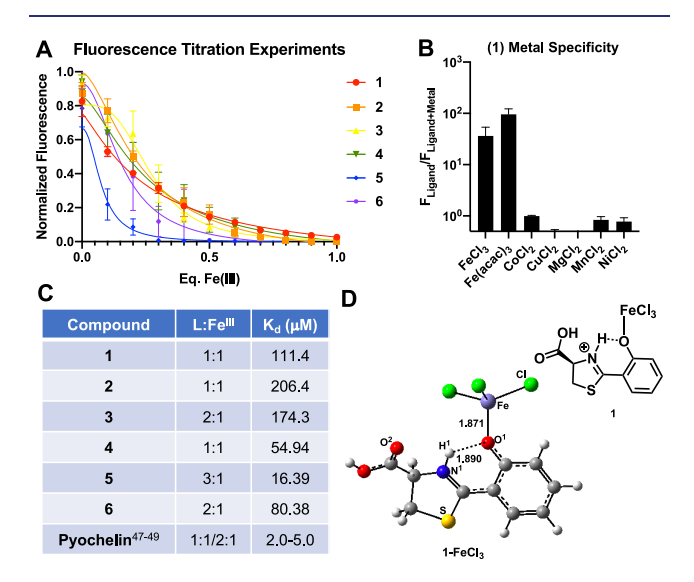


Figure 3. (A) Fluorescence titration curves of 1-6 titrated with 1.0 equiv of FeCl₃; (B) iron selectivity of 1; determined by dividing the starting fluorescence by the fluorescence after addition of 1.0 equiv of metal; (C) table of binding stoichiometries and calculated $K_{\rm d}$ values for 1-6 and pyochelin; $^{47-49}$ (D) ball-and-stick model of minimal energy structures of 1-FeCl₃ complex.

biologically relevant metals: cobalt, copper, magnesium, manganese, and nickel. Surprisingly, none quenched the emission signal, indicating that unlike pyochelin, ⁴⁶ the simplified structures of 1 and 2 both have a specific affinity for iron (Figures 3B, S2, and S3).

The ligand-to-Fe^{III} binding ratios (L:Fe^{III}) were next determined both experimentally and computationally (Figure 3C). Extrapolation of the emission quenching data found that compounds 1, 2, and 4 bound in a 1:1 complex with Fe^{III}, while 3, 5, and 6 bound in 2:1, 3:1, and 2:1 ratios, respectively. The L:Fe^{III} ratios for 1, 3, and 5 were further validated computationally (Figures 3D, S5, S6, and S7), thereby supporting our experimental L:Fe^{III} ratios (see Supporting Information). The emission quenching data were also used to calculate putative dissociation constant (K_d) values for 1-6, and all values were comparable to that of pyochelin (Figures 3C and S4).^{47–49} It should be noted that these calculated values are not absolute but simply serve as a benchmark estimate of the true K_d value of each ligand. These findings further support a potential physiological iron-binding role of these metabolites in *P. aeruginosa*.

On the basis of these results, we sought to perform a preliminary biological investigation of these metabolites to better understand the physiological ramifications, that is, do these compounds serve as growth promoters or inhibitors? Wild-type P. aeruginosa (PAO1) and a double knockout mutant, incapable of producing the native siderophores pyoverdine or pyochelin (Δ pvdD Δ pchEF), were incubated with each compound alone as well as prechelated with Fe^{III} in iron-depleted media, and growth to stationary phase was monitored (Figure 4). As expected, the unchelated compounds had a minimal effect on the growth of both PAO1 and Δ pvdD Δ pchEF, with the exception of **6**. In contrast, all of the prechelated compounds had a marked effect on rescuing the growth of both strains. In many cases, this enhancement of growth was greater than that resulting from incubation with the same concentration (125 μ M) of free Fe^{III}, indicating that growth is likely enhanced by the uptake of these ligand-Fe^{III} complexes. Additionally, as growth enhancements of both the wild-type and double mutant are similar, it is reasonable to assume that these complexes are being taken up directly into the cells without any recomplexation of iron with the native siderophores in PAO1.

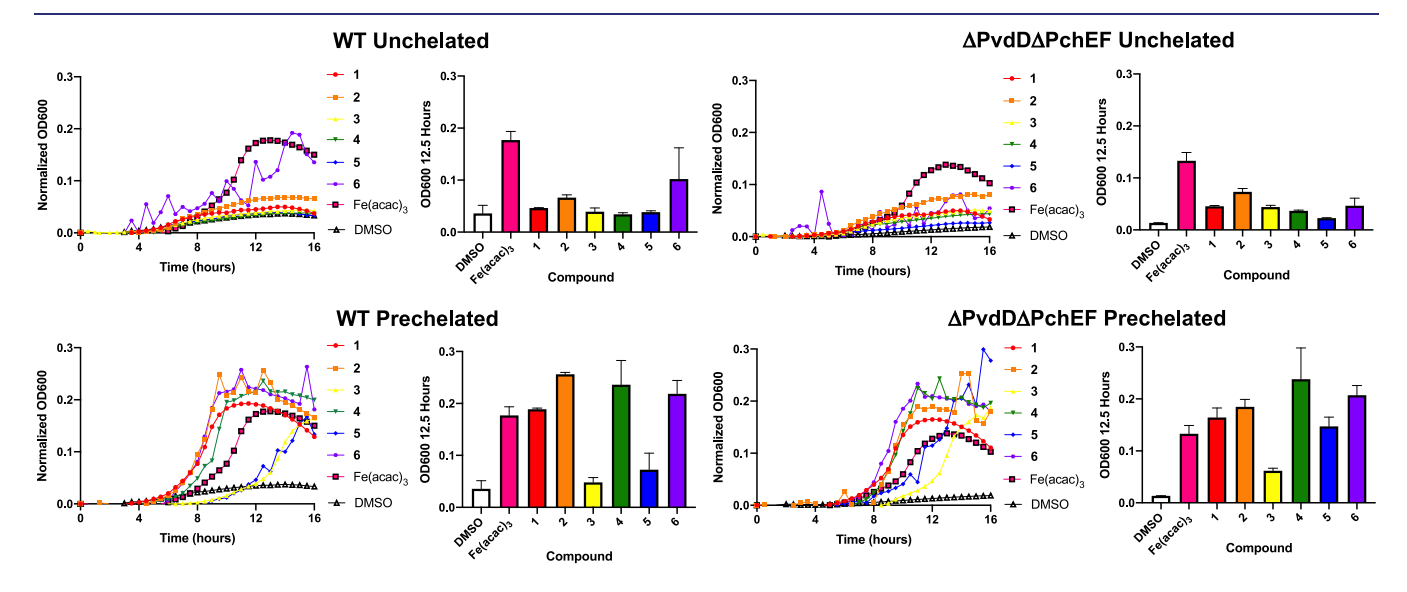


Figure 4. Growth curves of PAO1 (left) and Δ pvdD Δ pchEF (right) mutants with 125 μM of either prechelated ligand-iron complexes (top) and free ligand (bottom) and bar graphs showing the OD₆₀₀ value for each compound after 12.5 h of growth. Controls were Fe(acac)₃ and DMSO in all cases.

Interestingly, 3 and 5 both displayed delayed growth curves, in comparison to the other compounds tested. This may be due to delayed uptake of these two particular complexes, which differed in their ligand:iron ratios; however, further experimentation will be required to deduce the reason for this phenomenon. This biological data indicates, for the first time, that these simplified pyochelin-like molecules can act like siderophores, as the data indicate they are likely imported as complexes with Fe^{III}. While uptake of pyoverdine and pyochelin ferrisiderophore complexes is known to occur via TonB-dependent receptors, 36 it is unknown whether import of the Fe^{III} complexes of these simpler metabolites occurs via the same transport machinery or different receptor yet to be elucidated. Further work will be required to determine the transport machinery, if any, involved in complex uptake to confirm their role as siderophores.

These compounds were also tested for their ability to inhibit growth of various *Pseudomonads* (*P. fluorescens, P. putida, P. syringae*) and against a panel of other clinically relevant species (methicillin-resistant *Staphylococcus aureus, Enterococcus faecalis*, and *Escherichia coli*), but no growth inhibition was observed. The iron-binding properties of these compounds are therefore unlikely to play an inhibitory role through iron-chelation as is seen in the escherichelin-like mechanism.³¹

In this work, we sought to answer several questions about the physiochemical properties and biological role of several Pseudomonad metabolites arising from the Dha off-shoot pathway from the pyochelin biosynthetic machinery. Their iron-binding capabilities were extensively characterized and quantified both experimentally and computationally. In addition, siderophore-like properties were investigated. All ligand-iron complexes enhanced the growth of both the wildtype and $\Delta pvdD\Delta pchEF$ mutant grown in iron-depleted media. Further work will be required to fully elucidate the exact biological mechanism of these compounds including the related transport machinery. Looking forward, this work is likely to open new avenues of research to further study their biological roles, which may be siderophore-like mechanisms, but could also be a range of other functions. For example, their iron-binding properties may serve to function in a manner similar to the iron trapping mechnism displayed by PQS, another *Pseudomonad* metabolite.⁵⁰ Alternatively, it has been shown that pyochelin can act as a scavenger for hydroxyl radicals,⁵¹ meaning that metabolites such as aeruginol and IQS may be utilized as buffer compounds to relieve oxidative stress.²¹ Additionally, the antibiotic effects observed from the incorporation of IQS into the scaffolds of mindapyrrole B and malleonitrone suggest that perhaps some of these metabolites could be applied to a minimalist "Trojan-Horse" strategy utilized with many novel antibiotic compounds.⁵² However, it is also possible that these metabolites could simply be biosynthetic artifacts released through what has been previously identified as the "leaky hosepipe" mechanism,5 and the biological effects observed may not be representative of what occurs in nature. Therefore, future work elucidating the biological roles of these molecules is warranted.

METHODS

Metal Chelation Experiments. For the FeCl₃ titration assay, 1 mM stock solutions of each compound were titrated with differing volumes of 1 mM stock solution of FeCl₃ to give final test concentrations of 0 μ M, 125 μ M, 250 μ M, and 500 μ M. For the fluorescence titration assays, an emission

spectrum of 350 μ L of a 400 μ M stock solution of each compound in methanol was recorded ($\lambda_{\rm excitation}$ = wavelength of maximum absorbance ($\lambda_{\rm max}$), integration time = 1 s, accumulations = 10). A 10 mM stock solution of metal in methanol was added in 1.4 μ L portions (0.1 equiv) and the emission spectrum recorded after each addition. Fluorescence measurements were recorded on a FluoroMax spectrophotometer (Horiba Scientific, Edison, New Jersey). These measurements were taken in a quartz fluorescence cuvette with a 1 cm path length, a 258–550 nm integration range, and a 2 nm excitation and emission slit width.

Computational Analysis. Geometry optimizations and frequency calculations were performed with the Gaussian 09 suite of programs ⁵⁴ at the B3LYP-D3(BJ)/[6-31G(d,p) + Lanl2dz (Fe)] level of theory. B3LYP ⁵⁵⁻⁵⁷ density functional was used with Grimme's empirical dispersion correction (D3) ^{58,59} and Becke-Johnson (BJ)'s damping schemes. ⁶⁰ Frequency analysis was used to characterize each minimum with zero imaginary frequencies. Bulk solvent effects were incorporated in all calculations at the self-consistent reaction field polarizable continuum model (IEF-PCM) ⁶¹ level. The Gibbs free energies were calculated at 298.15 K and 1 atm in water as the solvent.

Biological Assays. For the growth assay, bacterial strains were grown from freezer stocks for 16 h at 200 rpm in 5 mL of MOPS (3-N-morpholino)propanesulfonic acid) minimal media at 37 $^{\circ}$ C. Overnight cultures were diluted 1:100 in 5 mL of fresh MOPS minimal media and grown at 37 °C, 200 rpm to a predetermined OD₆₀₀ reading reflective of exponential growth. Bacteria were then diluted in iron-depleted MOPS minimal media to a concentration of 0.004; then 100 μL was inoculated into each well of a flat-bottom 96-well plate (Corning 3370) containing test compounds giving a final test concentration of 125 μ M. Plates were then incubated with some shaking at 37 °C until bacteria reached stationary phase and OD₆₀₀ reading were taken every hour. For the IC₅₀ assay, bacterial strains were grown from freezer stocks for 16 h at 200 rpm in 10 mL of media (Mueller-Hinton (MH) Broth, Todd Hewitt Broth (THB), or Trypticase Soy Broth (TSB) at 37 or 30 °C. Overnight cultures were diluted 1:100 in 5 mL of corresponding fresh media and grown at 200 rpm at 37 or 30 $^{\circ}\text{C}$ to a predetermined OD_{600} reading reflective of exponential growth. Bacteria were then diluted to a concentration of 0.004; then 100 μ L was inoculated into each well of a flat-bottom 96well plate (Corning 3370) containing 100 mL of serially diluted compound solutions giving final test concentrations of 250 μ M to 1.25 μ M. Plated were then incubated statically at 37 or 30 °C for 24 h and OD reading were taken at this point. All biological assays were performed in triplicate from three separate overnight cultures and averaged.

Synthesis. Compounds were synthesized using well-known reaction conditions or previously published protocols. $^{26,42-45}$ All nonaqueous reactions were conducted in flame-dried glassware equipped with a stir bar under argon atmosphere using HPLC-grade solvents. $\rm Et_3N$ was freshly distilled from $\rm CaH_2$ prior to use. Thin-layer chromatography was performed on 250 $\mu \rm M$ Silicycle silica gel F-254 plates and visualized by fluorescence or staining using potassium permanganate or vanillin stains. Organic solutions were concentrated under reduced pressure on a Buchi Rotavapor R3 rotary evaporator. Chromatographic purification was accomplished using a Biotage flash chromatography purification system.

ASSOCIATED CONTENT

5 Supporting Information

The Supporting Information is available free of charge at https://pubs.acs.org/doi/10.1021/acsinfecdis.0c00897.

Synthetic procedures and spectral data, metal chelation assays, computational parameters, biological assays, supporting figures (PDF)

AUTHOR INFORMATION

Corresponding Author

William M. Wuest — Department of Chemistry, Emory University, Atlanta, Georgia 30322, United States; oorcid.org/0000-0002-5198-7744; Phone: 1-404-712-1143; Email: www.est@emory.edu

Authors

Anna R. Kaplan — Department of Chemistry, Emory University, Atlanta, Georgia 30322, United States

Djamaladdin G. Musaev — Department of Chemistry, Emory University, Atlanta, Georgia 30322, United States; Cherry L. Emerson Center for Scientific Computation, Emory University, Atlanta, Georgia 30322, United States;

orcid.org/0000-0003-1160-6131

Complete contact information is available at: https://pubs.acs.org/10.1021/acsinfecdis.0c00897

Author Contributions

A.R.K. and W.M.W. designed and performed all of the laboratory experiments. D.G.M. performed the computational calculations. A.R.K and W.M.W. wrote and edited the manuscript.

Funding

We are grateful to the NIH (GM119426, supported 30% of the costs) and the NSF (CHE2003692 for W.M.W. (supported 30% of the costs) and CHE0958205 for D.G.M. (supported 10% of the costs)) for funding and for the use of the resources of the Cherry Emerson Center for Scientific Computation and the NMR instrumentation (funded by CHE1531620) used in this work. In addition, A.R.K. acknowledges the National Science Foundation Pre-Doctoral Fellowship (DGE1937971, supported 30% of the costs). The content is solely the responsibility of the authors and does not necessarily represent the official views of the National Institutes of Health.

Notes

The authors declare no competing financial interest.

■ ACKNOWLEDGMENTS

We thank Prof. Steve Diggle (Georgia Tech) for the PA Δ pvdD Δ pchEF strain used in the study and Prof. Steve Diggle and Marvin Whiteley (Georgia Tech) for fruitful discussions.

REFERENCES

- (1) Barry, S. M., and Challis, G. L. (2009) Recent advances in siderophore biosynthesis. *Curr. Opin. Chem. Biol.* 13, 205–215.
- (2) Keohane, C. E., Steele, A. D., and Wuest, W. M. (2015) The Rhizosphere Microbiome: A Playground for Natural Product Chemists. *Synlett* 26, 2739–2744.
- (3) Miethke, M., and Marahiel, M. (2007) Siderophore-Based Iron Acquisition and Pathogen Control. *Microbiol. Mol. Biol. Rev.* 71, 413–451.

- (4) Khan, A., Singh, P., and Srivastava, A. (2018) Synthesis, nature and utility of universal iron chelator Siderophore: A review. *Microbiol. Res.* 212-213, 103–111.
- (5) Andrews, S. C., Robinson, A. K., and Rodriguez-Quinones, F. (2003) Bacterial iron homeostasis. *FEMS. Microbiol. Rev.* 27, 215–237.
- (6) Cornelis, P. (2010) Iron uptake and metabolism in Pseudomonads. *Appl. Microbiol. Biotechnol.* 86, 1637–1645.
- (7) Wuest, W. M., Sattely, E. S., and Walsh, C. T. (2009) Three Siderophores from One Bacterial Enzymatic Assembly Line. *J. Am. Chem. Soc.* 131, 5056–5057.
- (8) Crosa, J. H., and Walsh, C. T. (2002) Genetics and Assembly Line Enzymology of Siderophore Biosynthesis in Bacteria. *Microbiol. Mol. Biol. Rev.* 66, 223–249.
- (9) Porras-Alfaro, A., and Bayman, P. (2011) Hidden Fungi, Emergent Properties: Endophytes and Microbiomes. *Annu. Rev. Phytopathol.* 49, 291–315.
- (10) Haas, D., and Défago, G. (2005) Biological Control of Soil-Borne Pathogens by Fluorescent *Pseudomonads. Nat. Rev. Microbiol.* 3, 307–319.
- (11) Bhagirath, A. Y., Li, Y., Somayajula, D., Dadashi, M., Badr, S., and Duan, K. (2016) Cystic Fibrosis Lung Environment and Pseudomonas aeruginosa Infection. *BMC Pulm. Med.* 16, 17.
- (12) Leoni, L., Ciervo, A., Orsi, N., and Visca, P. (1996) Iron-Regulated Transcription of the *pvdA* Gene in *Pseudomonas aeruginosa*: Effect of Fur and PvdS on Promoter Activity. *J. Bacteriol.* 178, 2299–2313.
- (13) Igarashi, Y., Asano, D., Sawamura, M., In, Y., Ishida, T., and Imoto, M. (2016) Ulbactins F and G, Polycyclic Thiazoline Derivatives with Tumor Cell Migration Inhibitory Activity from *Brevibacillus* sp. *Org. Lett.* 18, 1658–1661.
- (14) Shapiro, J. A., Morrison, K. R., Chodisetty, S. S., Musaev, D. G., and Wuest, W. M. (2018) Biologically Inspired Total Synthesis of Ulbactin F, an Iron-Binding Natural Product. *Org. Lett.* 20, 5922–5926.
- (15) Li, W., Estrada-de los Sntos, P., Matthijs, S., Zie, G.-L., Busson, R., Cornelis, P., Roenski, J., and De Mot, R. (2011) Promysalin, a Salicylate-Containing *Pseudomonas putida* Antibiotic, Promotes Surface Colonization and Selectively Targets Other *Pseudomonas. Chem. Biol.* 18, 1320–1330.
- (16) Steele, A. D., Knouse, K. W., Keohane, C. E., and Wuest, W. M. (2015) Total Synthesis and Biological Investigation of (–)-Promysalin. *J. Am. Chem. Soc.* 137, 7314–7317.
- (17) Steele, A. D., Keohane, C. E., Knouse, K. W., Rossiter, S. E., Williams, S. J., and Wuest, W. M. (2016) Diverted Total Synthesis of Promysalin Analogs Demonstrates that an Iron-Binding Motif is Responsible for Its Narrow-Spectrum Antibacterial Activity. *J. Am. Chem. Soc.* 138, 5833–5836.
- (18) Keohane, C. E., Steele, A. D., Fetzer, C., Khowsathis, J., Van Tyne, D., Moynié, L., Gilmore, M. S., Karanicolas, J., Sieber, S. A., and Wuest, W. M. (2018) Promysalin Elicits Species-Selective Inhibition of *Pseudomonas aeruginosa* by Targeting Succinate Dehydrogenase. *J. Am. Chem. Soc.* 140, 1774–1782.
- (19) Serino, L., Reimmann, C., Visca, P., Beyeler, M., Chiesa, V. D., and Haas, D. (1997) Biosynthesis of Pyochelin and Dihydroaer-uginoic Acid Requires the Iron-Regulated *pch*DCBA Operon in *Pseudomonas aeruginosa. J. Bacteriol.* 179, 248–257.
- (20) Ronnebaum, T. A., and Lamb, A. L. (2018) Nonribosomal peptides for iron acquisition: pyochelin bioynthesis as a case study. *Curr. Opin. Struct. Biol.* 53, 1–11.
- (21) Ye, L., Cornelis, P., Guillemyn, K., Ballet, S., Christophersen, C., and Hammerich, O. (2014) Structure Revision of N-Mercapto-4-formylcarbostyril Produced by *Pseudomonas fluorescens* G308 to 2-(2-Hydroxyphenyl)thiazole-4-carbaldehyde [aeruginaldehyde]. *Nat. Prod. Commun.* 9, 789–794.
- (22) Mevers, E., Saurí, J., Helrich, E. J. N., Henke, M., Burns, K. J., Bugni, T. S., Andes, A., Curris, C. R., and Clardy, J. (2019) Pyonitrins A-D: Chimeric Natural Products Produced by *Pseudomonas protegens*. *J. Am. Chem. Soc.* 141, 17098–17101.

- (23) Trottmann, F., Franke, J., Ishida, K., García-Altares, M., and Hertweck, C. (2019) A Pair of Bacterial Siderophores Releases and Traps an Intercellular Signal Molecule: An Unusual Case of Natural Nitrone Bioconjugation. *Angew. Chem., Int. Ed.* 58, 200–204.
- (24) Elliot, G. T., Kelly, K. F., Bonna, R. L., Wardlaw, T. R., and Burns, E. R. (1988) In vitro antiproliferative activity of 2'-(2-hydroxyphenyl)-2'-thiazoline-4'-carboxylic acid and its methyl ester on L1210 and P388 murine neoplasms. *Cancer Chemother. Pharmacol.* 21, 233–236.
- (25) Carmi, R., Carmeli, S., et al. (1994) (+)-(S)-Dihydroaeruginoic Acid, an Inhibitor of *Septori tritici* and other phytopathogenic fungi and bacteria, produced by *Pseudomonas fluorescens. J. Nat. Prod.* 57, 1200–1205.
- (26) Yamada, Y., Seki, N., Kitahara, T., Takahashi, M., and Matsui, M. (1970) The Structure and Synthesis of Aeruginoic Acid (2-o-Hydroxy-phenylthiazole-4-carboxylic Acid). *Agric. Biol. Chem.* 34, 780–783
- (27) Yang, W., Dostal, L., and Rosazza, J. P. N. (1993) Aeruginol {2-(2'-hydroxyphenyl)-4-hydroxymethylthiazole}, a New Secondary Metabolite from *Pseudomonas aeruginosa*. *J. Nat. Prod.* 56, 1993–1994.
- (28) Lee, J. Y., Moon, S. S., and Hwang, B. K. (2003) Isolation and Antifungal and Antioomycete Activities of Aerugine Produced by *Pseudomonas fluorescens* Strain MM-B16. *Appl. Environ. Microbiol.* 69, 2023–2031.
- (29) Bukovits, G. J., Mohr, N. M., Budzikiewicz, H., Korth, H., and Pulverer, G. (1982) 2-Phenylthiazol-Derivate aus *Pseudomonas cepacia*. Z. Naturforsch., B: J. Chem. Sci. 37b, 877–880.
- (30) Fakhouri, W., Walker, F., Vogler, B., Armbruster, W., and Buchenauer, H. (2001) Isolation and identification of *N*-mercapto-4-formylcarbostyril, an antibiotic produced by *Pseudomonas fluorescens*. *Phytochemistry* 58, 1297–1303.
- (31) Lee, J., Wu, J., Deng, Y., Wang, J., Wang, C., Wang, J., Chang, C., Dong, Y., Williams, P., and Zhang, L.-H. (2013) A cell-cell communication signal integrates quorum sensing and stress response. *Nat. Chem. Biol.* 9, 339–343.
- (32) Cornelis, P. (2020) Putting an end to the *Pseudomonas* aeruginosa IQS controversy. *MicrobiologyOpen* 9, 1–2.
- (33) Lacerna, N. M., II, Miller, B. W., Lim, A. L., Tun, J. O., Robes, J. M. D., Cleofas, M. J. B., Lin, Z., Salvador-Reyes, L. A., Haygood, M. G., Schmidt, E. W., and Concepcion, G. P. (2019) Mindapyrroles A-C, Pyoluteorin Analogues from a Shipworm-Associated Bacterium. *J. Nat. Prod.* 82, 1024–1028.
- (34) Hammer, P. E., Hill, D. S., Lam, S. T., Van Pée, K.-H., and Ligon, J. (1997) Four Genes from *Pseudomonas fluorescens* That Encode the Biosynthesis of Pyrrolnitrin. *Appl. Environ. Microbiol.* 63, 2147–2154.
- (35) Shingare, R. D., Aniebok, V., Lee, H.-W., and MacMillan, J. B. (2020) Synthesis and Investigation of the Abiotic Formation of Pyonitrins A-D. *Org. Lett.* 22, 1516–1519.
- (36) Cornelis, P., and Dingemans, J. (2013) *Pseudomonas aeruginosa* adapts its iron uptake strategies in function of the type of infections. *Front. Cell. Infect. Microbiol.* 3, 1–7.
- (37) Reimmann, C., Serino, L., Beyeler, M., and Haas, D. (1998) Dihydroaeruginoic acid synthetase and pyochelin synthetase, products of the *pchEF* genes, are induced by extracellular pyochelin in *Pseudomonas aeruginosa*. *Microbiology* 144, 3135–3148.
- (38) Maspoli, A., Wenner, N., Mislin, G. L. A., and Reimmann, C. (2014) Functional analysis of pyochelin-/enantiopyochelin-related genes from a pathogenicity island of *Pseudomonas aeruginosa* strain PA14. *BioMetals* 27, 559–573.
- (39) Mislin, G. L. A., Hoegy, F., Cobessi, D., Poole, D. R., Schlk, I. J., et al. (2006) Binding Properties of Pyochelin and Structurally Related Molecules to FptA of *Pseudomonas aeruginosa*. *J. Mol. Biol.* 357, 1437–1448.
- (40) Ahmadi, M. K., Fawaz, S., Jones, C. H., Zhang, G., and Pfeifer, B. A. (2015) Total Biosynthesis and Diverse Applications of the Nonribosomal Peptide-Polyketide Siderophore Yersiniabactin. *Appl. Environ. Microbiol.* 81, 5290–5298.

- (41) Ohlemacher, S. I., Giblin, D. E., d'Avignon, D. A., Stapleton, A. E., Trautner, B. W., and Henderson, J. P. (2017) Enterobacteria secrete an inhibitor of *Pseudomonas* virulence during clinical bacteriuria. *J. Clin. Invest.* 127, 74018–74030.
- (42) Zamri, A., and Abdallah, A. (2000) An Improved Stereocontrolled Synthesis of Pyochelin, Siderophore of *Pseudomonas aeruginosa* and *Burkholderia cepacia*. *Tetrahedron* 56, 249–256.
- (43) Noël, S., Guillon, L., Schalk, I. J., and Mislin, G. L. A. T. (2011) Synthesis of Fluorescent Probes Based on the Pyochelin Siderophore Scaffold. *Org. Lett.* 13, 844–847.
- (44) Mislin, G. L., Burger, A., and Abdallah, M. A. (2004) Synthesis of new thiazole analogues of pyochelin, a siderophore of *Pseudomonas aeruginosa* and *Burkholderia cepacia*. A new conversion of thiazolines into thiazoles. *Tetrahedron 60*, 12139–12145.
- (45) Morrison, M. D., Hanthorn, J. J., and Pratt, D. A. (2009) Synthesis of Pyrrolnitrin and Related Halogenated Phenylpyrroles. *Org. Lett.* 11, 1051–1054.
- (46) Braud, A., Hannauer, M., Mislin, G. L. A., and Schalk, I. J. (2009) The *Pseudomonas aeruginosa* Pyochelin-Iron Uptake Pahway and Its Metal Specificity. *J. Bacteriol.* 191, 3517–3525.
- (47) Cox, C. D., and Graham, R. (1979) Isolation of an Iron-Binding Compound from *Pseudomonas aeruginosa. J. Bacteriol.* 137, 357–364. (48) Schlegel, K., Lex, J., Taraz, K., and Budzikiewicz, H. (2006) The X-Ray Structure of the Pyochelin Fe³⁺ Complex. *Z. Naturforsch., C: J. Biosci.* 61, 263–266.
- (49) Tseng, C.-F., Burger, A., Mislin, G. L. A., Schalk, I. S., Yu, S. S-F., Chan, S. I., and Abdallah, M. A. (2006) Bacterial siderophores: the solution stoichiometry and coordination of the Fe(III) complexes of pyochelin and related compounds. *JBIC, J. Biol. Inorg. Chem.* 11, 419–432.
- (50) Diggle, S. P., Matthijs, S., Wright, V. J., Fletcher, M. P., Chhabra, S. R., Lamont, I. L., Kong, Z., Hider, R. C., Cornelis, P., Cámara, M., and Williams, P. (2007) The *Pseudomonas aeruginosa* 4-Quinolone Signal Molecules HHQ and PQS Play Multifunctional Roles in Quoru Sensing and Iron Entrapment. *Chem. Biol.* 14, 87–96.
- (51) Coffman, T. J., Cox, C. D., Edeker, B. L., and Britigan, B. E. (1990) Possible role of bacterial siderophores in inflammation. Iron bound to the *Pseudomonas* siderophore pyochelin can function as a hydroxyl radical catalyst. *J. Clin. Invest.* 86, 1030–1037.
- (52) Cheng, A. V., and Wuest, W. M. (2019) Signed, Sealed, Delivered: Conjugate and Prodrug Strategies as Targeted Delivery Vectors for Antibiotics. *ACS Infect. Dis. 5*, 816–828.
- (53) Wu, J., Hothersall, J., Mazzetti, C., O'Connell, Y., Shields, J. A., Rahman, A. S., Cox, R. J., Crosby, J., Simpson, T. J., Thomas, C. M., and Willis, C. L. (2008) In vivo Mutational Analysis of the Mupirocin Gene Cluster Reveals Labile Points in the Biosynthetic Pathway: the "Leaky Hosepipe" Mechanism. *ChemBioChem* 9, 1500–1508.
- (54) Frisch, M. J., Trucks, G. W., Schlegel, H. B., Scuseria, G. E., Robb, M. A., Cheeseman, J. R., Scalmani, G., Barone, V., Mennucci, B., Petersson, G. A., Nakatsuji, H., Caricato, M., Li, X., Hratchian, H. P., Izmaylov, A. F., Bloino, J., Zheng, G., Sonnenberg, J. L., Hada, M., Ehara, M., Toyota, K., Fukuda, R., Hasegawa, J., Ishida, M., Nakajima, T., Honda, Y., Kitao, O., Nakai, H., Vreven, T., Montgomery, J. A., Jr., Peralta, J. E., Ogliaro, F., Bearpark, M., Heyd, J. J., Brothers, E., Kudin, K. N., Staroverov, V. N., Kobayashi, R., Normand, J., Raghavachari, K., Rendell, A., Burant, J. C., Iyengar, S. S., Tomasi, J., Cossi, M., Rega, N., Millam, J. M., Klene, M., Knox, J. E., Cross, J. B., Bakken, V., Adamo, C., Jaramillo, J., Gomperts, R., Stratmann, R. E., Yazyev, O., Austin, A. J., Cammi, R., Pomelli, C., Ochterski, J. W., Martin, R. L., Morokuma, K., Zakrzewski, V. G., Voth, G. A., Salvador, P., Dannenberg, J. J., Dapprich, S., Daniels, A. D., Farkas, O., Foresman, J. B., Ortiz, J. V., Cioslowski, J., and Fox, D. J. Gaussian 09, revision D.01; Gaussian, Inc.: Wallingford, CT, 2009.
- (55) Becke, A. D. (1988) Density-functional exchange-energy approximation with correct asymptotic behavior. *Phys. Rev. A: At., Mol., Opt. Phys.* 38, 3098–3100.
- (56) Lee, C., Yang, W., and Parr, R. G. (1988) Development of the Cole-Salvetti correlation-energy formula into a functional of the

electron density. Phys. Rev. B: Condens. Matter Mater. Phys. 37, 785-789

- (57) Becke, D. (1993) A new mixing of Hartree-Fock and local density-functional theories. *J. Chem. Phys.* 98, 1372–1377.
- (58) Grimme, S., Antony, J., Ehrlich, S., and Krieg, H. (2010) A consistent and accurate ab initio parametrization of density functional dispersion correction (DFT-D) for the 94 elements H-Pu. *J. Chem. Phys.* 132, 154104.
- (59) Grimme, S., Hansen, A., Brandenburg, J. G., and Bannwarth, C. (2016) Dispersion-corrected mean-field electronic structure methods. *Chem. Rev.* 116, 5105–5154.
- (60) Becke, A. D., and Johnson, E. R. (2005) Exchange-hole dipole moment and the dispersion interaction. *J. Chem. Phys.* 122, 154104.
- (61) Cancès, E., Mennucci, B., and Tomasi, J. (1997) A new integral equation formalism for the polarizable continuum model: Theoretical background and applications to isotropic and anisotropic dielectrics. *J. Chem. Phys.* 107, 3032–3041.